LA-UR-17-30851
Approved for public release; distribution is unlimited.

Title: (U) Second-Order Sensitivity Analysis of Uncollided Particle Contributions to Radiation Detector Responses Using Ray-Tracing

Author(s): Favorite, Jeffrey A.

Intended for: Report

Issued: 2017-11-30

Los Alamos
NATIONAL LABORATORY

memorandum

X-Computational Physics Division
Monte Carlo Methods, Codes, and Applications Group

Group XCP-3, MS F663
Los Alamos, New Mexico 87545
505/667-1920

To/MS: Distribution
From/MS: Jeffrey A. Favorite / XCP-3, MS F663
Phone/Email: 7-7941 / fave@lanl.gov
Symbol: XCP-3:17–059(U) (LA–UR–17–?????)
Date: November 28, 2017

SUBJECT: (U) Second-Order Sensitivity Analysis of Uncollided Particle Contributions to Radiation Detector Responses Using Ray-Tracing

I. Introduction

The Second-Level Adjoint Sensitivity System (2nd-LASS) that yields the second-order sensitivities of a response of uncollided particles with respect to isotope densities, cross sections, and source emission rates is derived in Refs. 1 and 2. In Ref. 2, we solved problems for the uncollided leakage from a homogeneous sphere and a multiregion cylinder using the PARTISN multigroup discrete-ordinates code.[3] In this memo, we derive solutions of the 2nd-LASS for the particular case when the response is a flux or partial current density computed at a single point on the boundary, and the inner products are computed using ray-tracing.[4,5,6] Both the PARTISN approach and the ray-tracing approach are implemented in a computer code, SENSPG.

The next section of this report presents the equations of the 1st- and 2nd-LASS for uncollided particles and the first- and second-order sensitivities that use the solutions of the 1st- and 2nd-LASS. Section III presents solutions of the 1st- and 2nd-LASS equations for the case of ray-tracing from a detector point. Section IV presents specific solutions of the 2nd-LASS and derives the ray-trace form of the inner products needed for second-order sensitivities. Numerical results for the total leakage from a homogeneous sphere are presented in Sec. V and for the leakage from one side of a two-region slab in Sec. VI. Section VII is a summary and conclusions.

II. Equations of the 1st- and 2nd-LASS for Uncollided Particles

This section summarizes results derived by Cacuci.[1]

II.A. 1st LASS

The forward equation in the 1st LASS is

$$\mathbf{\Omega}\cdot\nabla\varphi(\mathbf{r},\mathbf{\Omega})+\Sigma_t(\mathbf{r})\varphi(\mathbf{r},\mathbf{\Omega})=\frac{q(\mathbf{r})}{4\pi} \tag{1}$$

with the vacuum boundary condition

$$\varphi(\mathbf{r}_s,\mathbf{\Omega})=0,\ \mathbf{r}_s\in\partial V,\ \mathbf{\Omega}\cdot\mathbf{n}<0. \tag{2}$$

The adjoint equation in the 1st LASS is

$$-\mathbf{\Omega}\cdot\nabla\psi^{(1)}(\mathbf{r},\mathbf{\Omega})+\Sigma_t(\mathbf{r})\psi^{(1)}(\mathbf{r},\mathbf{\Omega})=\Sigma_d(\mathbf{r},\mathbf{\Omega}) \tag{3}$$

with the vacuum boundary condition

$$\psi^{(1)}(\mathbf{r}_s,\mathbf{\Omega})=0,\ \mathbf{r}_s\in\partial V,\ \mathbf{\Omega}\cdot\mathbf{n}>0. \tag{4}$$

First-order sensitivities of a response R with respect to the N_m isotope number densities, cross sections, and source emission rates are given by inner products of the solutions of the 1st-LASS:

$$\begin{aligned} S_i^{(1)}(\varphi,\boldsymbol{\alpha};\psi^{(1)}) \triangleq \frac{\partial R}{\partial N_i} &= -\sigma_i\int dV\int_{4\pi}d\mathbf{\Omega}\, f_i(\mathbf{r})\psi^{(1)}(\mathbf{r},\mathbf{\Omega})\varphi(\mathbf{r},\mathbf{\Omega}) \\ &\quad + q_i\int dV\int_{4\pi}d\mathbf{\Omega}\,\psi^{(1)}(r,\mathbf{\Omega})g_i(\mathbf{r}),\ i=1,...,N_m; \end{aligned} \tag{5}$$

$$S_{i+N_m}^{(1)}(\varphi,\boldsymbol{\alpha};\psi^{(1)}) \triangleq \frac{\partial R}{\partial \sigma_i} = -N_i\int dV\int_{4\pi}d\mathbf{\Omega}\, f_i(\mathbf{r})\psi^{(1)}(\mathbf{r},\mathbf{\Omega})\varphi(\mathbf{r},\mathbf{\Omega}),\ i=1,...,N_m; \tag{6}$$

$$S_{i+2N_m}^{(1)}(\boldsymbol{\alpha};\psi^{(1)}) \triangleq \frac{\partial R}{\partial q_i} = N_i\int dV\int_{4\pi}d\mathbf{\Omega}\,\psi^{(1)}(\mathbf{r},\mathbf{\Omega})g_i(\mathbf{r}),\ i=1,...,N_m. \tag{7}$$

In Eqs. (5), (6), and (7), $f_i(\mathbf{r})$ and $g_i(\mathbf{r})$ represent the piecewise spatially constant distributions of the cross sections and source emission rates, respectively, of isotope *i*. The density derivatives here and everywhere in this paper are constant-volume partial derivatives.[7]

II.B. 2nd-LASS Equations for Second-Order Sensitivities $S_{i,j}^{(2)} \triangleq \dfrac{\partial^2 R}{\partial N_i \partial \alpha_j},\ i=1,...,N_m,\ j=1,...,N_m$

The 2nd-level adjoint functions $\psi_{1,i}^{(2)}$ and $\psi_{2,i}^{(2)}$ are the solutions of the following 2nd-LASS:

$$\mathbf{\Omega}\cdot\nabla\psi_{1,i}^{(2)}(\mathbf{r},\mathbf{\Omega})+\Sigma_t(\mathbf{r})\psi_{1,i}^{(2)}(\mathbf{r},\mathbf{\Omega})=-\sigma_i f_i(\mathbf{r})\varphi(\mathbf{r},\mathbf{\Omega})+q_i g_i(\mathbf{r}),\quad i=1,...,N_m, \tag{8}$$

$$\psi_{1,i}^{(2)}(\mathbf{r}_s,\mathbf{\Omega})=0,\ \mathbf{r}_s\in\partial V,\ \mathbf{\Omega}\cdot\mathbf{n}<0, \tag{9}$$

$$-\mathbf{\Omega}\cdot\nabla\psi_{2,i}^{(2)}(\mathbf{r},\mathbf{\Omega})+\Sigma_t(\mathbf{r})\psi_{2,i}^{(2)}(\mathbf{r},\mathbf{\Omega})=-\sigma_i f_i(\mathbf{r})\psi^{(1)}(\mathbf{r},\mathbf{\Omega}),\ i=1,...,N_m, \tag{10}$$

$$\psi_{2,i}^{(2)}(\mathbf{r}_s,\mathbf{\Omega})=0,\ \mathbf{r}_s\in\partial V,\ \mathbf{\Omega}\cdot\mathbf{n}>0. \tag{11}$$

The 2nd-order mixed partial sensitivities (that include N_i) of the response R with respect to the model parameters are

$$\begin{aligned} S_{i,j}^{(2)} \triangleq \frac{\partial^2 R}{\partial N_i\partial N_j} &= -\sigma_j\int dV\int_{4\pi}d\mathbf{\Omega}\left[\psi_{1,i}^{(2)}(\mathbf{r},\mathbf{\Omega})\psi^{(1)}(\mathbf{r},\mathbf{\Omega})+\psi_{2,i}^{(2)}(\mathbf{r},\mathbf{\Omega})\varphi(\mathbf{r},\mathbf{\Omega})\right]f_j(\mathbf{r}) \\ &\quad + q_j\int dV\int_{4\pi}d\mathbf{\Omega}\,\psi_{2,i}^{(2)}(\mathbf{r},\mathbf{\Omega})g_j(\mathbf{r}),\quad i,j=1,...,N_m, \end{aligned} \tag{12}$$

$$\begin{aligned} S_{i,j+N_m}^{(2)} \triangleq \frac{\partial^2 R}{\partial N_i\partial \sigma_j} &= -N_j\int dV\int_{4\pi}d\mathbf{\Omega}\left[\psi_{1,i}^{(2)}(\mathbf{r},\mathbf{\Omega})\psi^{(1)}(\mathbf{r},\mathbf{\Omega})+\psi_{2,i}^{(2)}(\mathbf{r},\mathbf{\Omega})\varphi(\mathbf{r},\mathbf{\Omega})\right]f_j(\mathbf{r}) \\ &\quad - \delta_{ij}\int dV\int_{4\pi}d\mathbf{\Omega}\, f_i(\mathbf{r})\psi^{(1)}(\mathbf{r},\mathbf{\Omega})\varphi(\mathbf{r},\mathbf{\Omega}),\quad i,j=1,...,N_m, \end{aligned} \tag{13}$$

$$\begin{aligned} S_{i,j+2N_m}^{(2)} \triangleq \frac{\partial^2 R}{\partial N_i\partial q_j} &= N_j\int dV\int_{4\pi}d\mathbf{\Omega}\,\psi_{2,i}^{(2)}(\mathbf{r},\mathbf{\Omega})g_j(\mathbf{r})+\delta_{ij}N_j\int dV\int_{4\pi}d\mathbf{\Omega}\, g_i(\mathbf{r})\psi^{(1)}(\mathbf{r},\mathbf{\Omega}), \\ &\quad i,j=1,...,N_m. \end{aligned} \tag{14}$$

II.C. 2nd-LASS Equations for Second-Order Sensitivities $S^{(2)}_{i+N_m,j} \triangleq \dfrac{\partial^2 R}{\partial\sigma_i\partial\alpha_j},\ i=1,...,N_m,\ j=1,...,N_m$

The 2nd-level adjoint functions $\psi^{(2)}_{1,i+N_m}$ and $\psi^{(2)}_{2,i+N_m}$ are the solutions of the following 2nd-LASS:

$$\mathbf{\Omega}\cdot\nabla\psi^{(2)}_{1,i+N_m}(\mathbf{r},\mathbf{\Omega})+\Sigma_t(\mathbf{r})\psi^{(2)}_{1,i+N_m}(\mathbf{r},\mathbf{\Omega})=-N_i f_i(\mathbf{r})\varphi(\mathbf{r},\mathbf{\Omega}),\ i=1,...,N_m, \tag{15}$$

$$\psi^{(2)}_{1,i+N_m}(\mathbf{r}_s,\mathbf{\Omega})=0,\ \ \mathbf{r}_s\in\partial V,\ \ \mathbf{\Omega}\cdot\mathbf{n}<0, \tag{16}$$

$$-\mathbf{\Omega}\cdot\nabla\psi^{(2)}_{2,i+N_m}(\mathbf{r},\mathbf{\Omega})+\Sigma_t(\mathbf{r})\psi^{(2)}_{2,i+N_m}(\mathbf{r},\mathbf{\Omega})=-N_i f_i(\mathbf{r})\psi^{(1)}(\mathbf{r},\mathbf{\Omega}),\ i=1,...,N_m, \tag{17}$$

$$\psi^{(2)}_{2,i+N_m}(\mathbf{r}_s,\mathbf{\Omega})=0,\ \mathbf{r}_s\in\partial V,\ \mathbf{\Omega}\cdot\mathbf{n}>0. \tag{18}$$

The 2nd-order mixed partial sensitivities (that include σ_i) of the response R with respect to the model parameters are

$$\begin{aligned}S^{(2)}_{i+N_m,j}&\triangleq\frac{\partial^2 R}{\partial\sigma_i\partial N_j}=-\sigma_j\int dV\int_{4\pi}d\mathbf{\Omega}\Big[\psi^{(2)}_{1,i+N_m}(\mathbf{r},\mathbf{\Omega})\psi^{(1)}(\mathbf{r},\mathbf{\Omega})+\psi^{(2)}_{2,i+N_m}(\mathbf{r},\mathbf{\Omega})\varphi(\mathbf{r},\mathbf{\Omega})\Big]f_j(\mathbf{r})\\&+q_j\int dV\int_{4\pi}d\mathbf{\Omega}\,\psi^{(2)}_{2,i+N_m}(\mathbf{r},\mathbf{\Omega})g_j(\mathbf{r})-\delta_{ij}\int dV\int_{4\pi}d\mathbf{\Omega}\,f_i(\mathbf{r})\psi^{(1)}(\mathbf{r},\mathbf{\Omega})\varphi(\mathbf{r},\mathbf{\Omega}),\quad i,j=1,...,N_m,\end{aligned} \tag{19}$$

$$\begin{aligned}S^{(2)}_{i+N_m,j+N_m}&\triangleq\frac{\partial^2 R}{\partial\sigma_i\partial\sigma_j}\\&=-N_j\int dV\int_{4\pi}d\mathbf{\Omega}\Big[\psi^{(2)}_{1,i+N_m}(\mathbf{r},\mathbf{\Omega})\psi^{(1)}(\mathbf{r},\mathbf{\Omega})+\psi^{(2)}_{2,i+N_m}(\mathbf{r},\mathbf{\Omega})\varphi(\mathbf{r},\mathbf{\Omega})\Big]f_j(\mathbf{r}),\ i,j=1,...,N_m,\end{aligned} \tag{20}$$

$$S^{(2)}_{i+N_m,j+2N_m}\triangleq\frac{\partial^2 R}{\partial\sigma_i\partial q_j}=N_j\int dV\int_{4\pi}d\mathbf{\Omega}\psi^{(2)}_{2,i+N_m}(\mathbf{r},\mathbf{\Omega})g_j(\mathbf{r}),\quad i,j=1,...,N_m. \tag{21}$$

II.D. 2nd-LASS Equations for Second-Order Sensitivities $S^{(2)}_{i+2N_m,j}\triangleq\dfrac{\partial^2 R}{\partial q_i\partial\alpha_j},\ i=1,...,N_m,\ j=1,...,N_m$

The 2nd-level adjoint function $\psi^{(2)}_{1,i+2N_m}$ is the solution of the following 2nd-LASS:

$$\mathbf{\Omega}\cdot\nabla\psi^{(2)}_{1,i+2N_m}(\mathbf{r},\mathbf{\Omega})+\Sigma_t(\mathbf{r})\psi^{(2)}_{1,i+2N_m}(\mathbf{r},\mathbf{\Omega})=N_i\,g_i(\mathbf{r}),\ i=1,...,N_m, \tag{22}$$

$$\psi^{(2)}_{1,i+2N_m}(\mathbf{r}_s,\mathbf{\Omega})=0,\ \mathbf{r}_s\in\partial V,\ \mathbf{\Omega}\cdot\mathbf{n}<0. \tag{23}$$

Note also that $\psi^{(2)}_{2,i+2N_m}\equiv 0$. The 2nd-order mixed partial sensitivities (that include q_i) of the response R with respect to the model parameters are

$$\begin{aligned}S^{(2)}_{i+2N_m,j}&\triangleq\frac{\partial^2 R}{\partial q_i\partial N_j}=-\sigma_j\int dV\int_{4\pi}d\mathbf{\Omega}\,\psi^{(2)}_{1,i+2N_m}(\mathbf{r},\mathbf{\Omega})\psi^{(1)}(\mathbf{r},\mathbf{\Omega})f_j(\mathbf{r})\\&+\delta_{ij}\int dV\int_{4\pi}d\mathbf{\Omega}\,\psi^{(1)}(\mathbf{r},\mathbf{\Omega})g_i(\mathbf{r}),\quad i,j=1,...,N_m,\end{aligned} \tag{24}$$

$$S^{(2)}_{i+2N_m,j+N_m}\triangleq\frac{\partial^2 R}{\partial q_i\partial\sigma_j}=-N_j\int dV\int_{4\pi}d\mathbf{\Omega}\,\psi^{(2)}_{1,i+2N_m}(\mathbf{r},\mathbf{\Omega})\psi^{(1)}(\mathbf{r},\mathbf{\Omega})f_j(\mathbf{r}),\quad i,j=1,...,N_m, \tag{25}$$

$$S^{(2)}_{i+2N_m,j+2N_m}\triangleq\frac{\partial^2 R}{\partial q_i\partial q_j}=0,\quad i,j=1,...,N_m. \tag{26}$$

III. Solutions of the 1st- and 2nd-LASS for Ray-Tracing from a Point Detector

III.A. 1st-LASS Forward Equation

Identify $\mathbf{\Omega}\cdot\nabla\varphi(\mathbf{r},\mathbf{\Omega})$ as the directional derivative of $\varphi(\mathbf{r},\mathbf{\Omega})$ at $\mathbf{r}$ in direction $\mathbf{\Omega}$.[8] Then Eq. (1) can be written[5]

$$\frac{\partial\varphi(r,\mathbf{\Omega})}{\partial r}+\Sigma_t(r)\varphi(r,\mathbf{\Omega})=\frac{q(r)}{4\pi}, \tag{27}$$

where r measures the distance along the ray in direction $\mathbf{\Omega}$. Equation (27) is equivalent to Eq. (1) provided that an arbitrary point in space $\mathbf{r}$ can be mapped to a unique point r along the unique ray in direction $\mathbf{\Omega}$ that passes through $\mathbf{r}$.

For this application, we only solve for particle directions that intersect a detector point $\mathbf{r}_d$ on the system boundary. Thus, for this application, a ray-trace solution of Eq. (1) is not a full solution for all points $\mathbf{r}$ and angles $\mathbf{\Omega}$. It is a solution for all points $\mathbf{r}$ but only certain angles, designated $\mathbf{\Omega}_d$ to emphasize that they are the angles along which rays intersect the detector. It is possible to solve Eq. (1) at an arbitrary point $\mathbf{r}$ and angle $\mathbf{\Omega}$ using ray-tracing, but that solution will not be derived or used here.

Assuming the medium is composed of homogeneous regions k with cross section and source rate density $\Sigma_{t,k}$ and q_k, respectively, Eq. (27) is (for the subset of angles $\mathbf{\Omega}_d$)

$$\frac{\partial\varphi(r,\mathbf{\Omega}_d)}{\partial r}+\Sigma_{t,k}\varphi(r,\mathbf{\Omega}_d)=\frac{q_k}{4\pi},\quad k=1,\ldots,K, \tag{28}$$

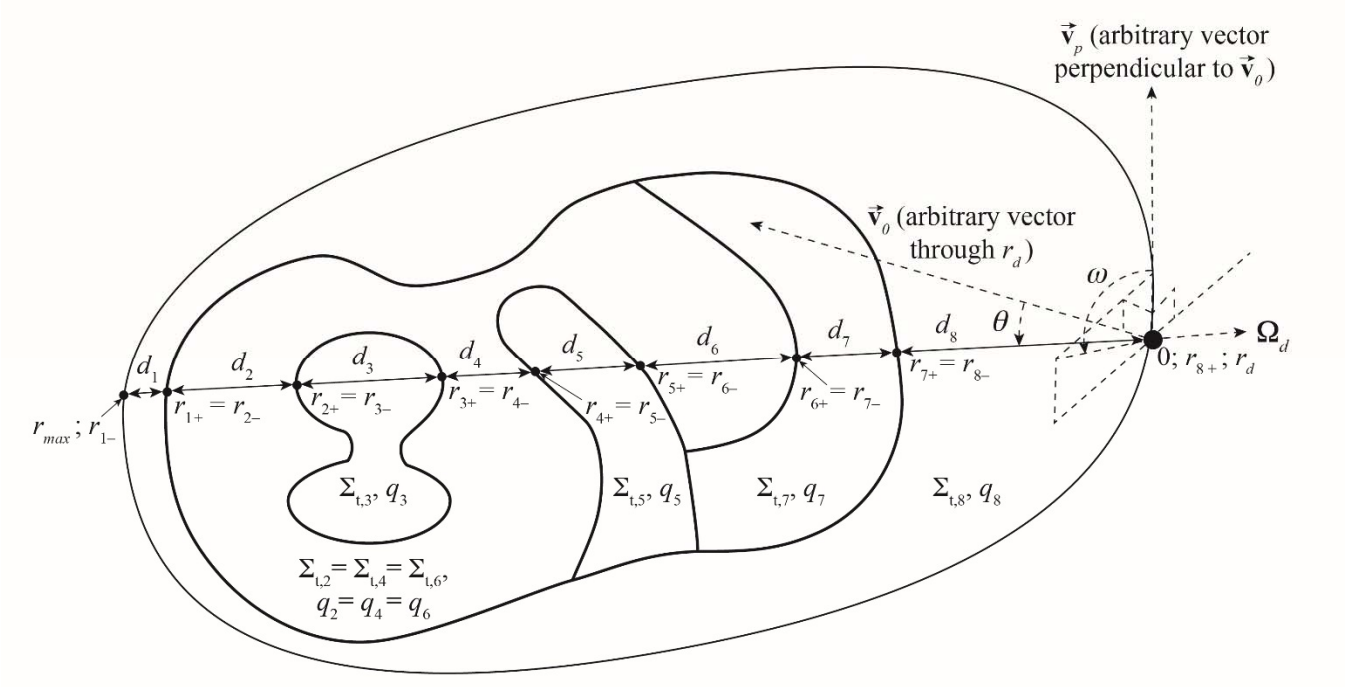

Figure 1. Ray-tracing in an arbitrary geometry. Adapted from Ref. 4. Copyright 2009 by the American Nuclear Society, LaGrange Park, Illinois.

where r is the distance along the ray in direction $\mathbf{\Omega}_d$ and K is the number of homogeneous regions the ray transits (*not* the number of homogeneous regions in the medium). Multiple traverses of a single region are counted separately. See Fig. 1, in which $K = 8$ for the ray shown.

Applying the integrating factor $e^{\Sigma_{t,k}(r-r_{k-})}$ yields

$$\frac{\partial}{\partial r}\left(e^{\Sigma_{t,k}(r-r_{k-})}\varphi(r,\mathbf{\Omega}_d)\right) = e^{\Sigma_{t,k}(r-r_{k-})}\frac{q_k}{4\pi}. \tag{29}$$

Clearly, the distance $r - r_{k-}$ depends on the angles θ and ω defining $\mathbf{\Omega}_d$ (see Fig. 1), so the functional dependence is suppressed. Integrating Eq. (29) yields

$$\begin{aligned} e^{\Sigma_{t,k}(r-r_{k-})}\varphi(r,\mathbf{\Omega}_d) &= \frac{q_k}{4\pi}\int dr\, e^{\Sigma_{t,k}(r-r_{k-})} + C \\ &= \frac{q_k}{4\pi\,\Sigma_{t,k}} e^{\Sigma_{t,k}(r-r_{k-})} + C. \end{aligned} \tag{30}$$

Dividing through by the integrating factor yields

$$\varphi(r,\mathbf{\Omega}_d) = \frac{q_k}{4\pi\,\Sigma_{t,k}} + C\,e^{-\Sigma_{t,k}(r-r_{k-})}. \tag{31}$$

Designate the 1st-LASS forward flux entering region k in direction $\mathbf{\Omega}_d$ as $\varphi(r_{k-},\mathbf{\Omega}_d)$. Using $r = r_{k-}$ in Eq. (31) and rearranging yields

$$C = \varphi(r_{k-},\mathbf{\Omega}_d) - \frac{q_k}{4\pi\,\Sigma_{t,k}}. \tag{32}$$

Using Eq. (32) in Eq. (31) and rearranging yields

$$\varphi(r,\mathbf{\Omega}_d) = \frac{q_k}{4\pi\,\Sigma_{t,k}}\left(1 - e^{-\Sigma_{t,k}(r-r_{k-})}\right) + \varphi(r_{k-},\mathbf{\Omega}_d)\,e^{-\Sigma_{t,k}(r-r_{k-})}. \tag{33}$$

The boundary condition, given by applying Eq. (2) to Fig. 1, completes the solution:

$$\varphi(r_{1-},\mathbf{\Omega}_d) = 0. \tag{34}$$

For Eq. (27), the boundary is the point at which the ray enters the system in direction $\mathbf{\Omega}_d$.

The quantity of interest is a detector response, denoted as $R(\varphi,\boldsymbol{\alpha})$, where $\boldsymbol{\alpha}$ denotes the vector of input parameters, of the form

$$R(\varphi,\boldsymbol{\alpha}) = \int dV \int_{4\pi} d\mathbf{\Omega}\; \Sigma_d(\mathbf{r},\mathbf{\Omega})\,\varphi(\mathbf{r},\mathbf{\Omega}), \tag{35}$$

where $\Sigma_d(\mathbf{r},\mathbf{\Omega})$ models the interaction of the detector with the incident particles. Detector responses of particular interest are: (i) the scalar flux at a point, in which case the detector-interaction function has the form

$$\Sigma_d(\mathbf{r},\mathbf{\Omega}) = \delta(\mathbf{r} - \mathbf{r}_d), \tag{36}$$

where $\mathbf{r}_d$ represents the detector's location, and (ii) the partial current density at a point, in which case the detector-interaction function has the form

$$\Sigma_d(\mathbf{r},\mathbf{\Omega}) = \mathbf{\Omega}\cdot\mathbf{n}\,\delta(\mathbf{r} - \mathbf{r}_d), \tag{37}$$

where $\mathbf{n}$ is a unit vector normal to the unit area at $\mathbf{r}_d$ through which the partial current density is to be calculated. Although Eq. (35) is an integral over all angles (4π), only those rays passing through $\mathbf{r}_d$ will contribute.

III.B. 1st-LASS Adjoint Equation

In the adjoint case, Eqs. (3) and (4), source particles *only* flow towards the detector point $\mathbf{r}_d$. Thus, for this application, a ray-trace solution of Eq. (3) is a full solution for all points $\mathbf{r}$ and angles $\mathbf{\Omega}$. Nevertheless, we continue to denote the angle as $\mathbf{\Omega}_d$ to emphasize that we only consider angles along which rays intersect the detector point.

Considering only angles that intersect the detector point, noting that adjoint particles travel backwards, and recognizing that the adjoint source within the system volume is zero [Eqs. (36) and (37)], Eq. (3) is written (for the subset of angles $\mathbf{\Omega}_d$)

$$\frac{\partial \psi^{(1)}(r,\mathbf{\Omega}_d)}{\partial r} + \Sigma_{t,k}\psi^{(1)}(r,\mathbf{\Omega}_d) = 0, \quad k = 1,\ldots,K, \tag{38}$$

where r is the distance along the ray in direction $-\mathbf{\Omega}_d$ and K is the number of homogeneous regions the ray transits. Designating the 1st-LASS adjoint flux entering region k in direction $-\mathbf{\Omega}_d$ as $\psi^{(1)}(r_{k+},\mathbf{\Omega}_d)$, the solution of Eq. (38) is

$$\psi^{(1)}(r,\mathbf{\Omega}_d) = e^{-\Sigma_{t,k}(r-r_{k+})}\psi^{(1)}(r_{k+},\mathbf{\Omega}_d). \tag{39}$$

Clearly, the distance $r - r_{k+}$ depends on the angles θ and ω defining $\mathbf{\Omega}_d$ (see Fig. 1), so the functional dependence is suppressed. The boundary condition, given by applying Eqs. (36) and (37) to Fig. 1, completes the solution:

$$\psi^{(1)}(r_{K+},\mathbf{\Omega}_d) = \frac{\Sigma_d\left(r_{K+},\mathbf{\Omega}_d\right)}{\left|\mathbf{\Omega}_d \cdot \mathbf{n}\right|}. \tag{40}$$

For Eq. (38), the boundary is the point at which the ray enters the system in direction $-\mathbf{\Omega}_d$.

The response $R(\varphi,\boldsymbol{\alpha})$ is also given by the dual of Eq. (35):[9]

$$R(\varphi,\boldsymbol{\alpha}) = \int dV \int_{4\pi} d\mathbf{\Omega}\,\psi^{(1)}(\mathbf{r},\mathbf{\Omega})\frac{q(\mathbf{r})}{4\pi}. \tag{41}$$

Although Eq. (41) is an integral over all angles (4π), the adjoint flux is only nonzero for angles $\mathbf{\Omega}_d$. Thus, only those rays passing through $\mathbf{r}_d$ will contribute to the response, as for Eq. (35).

III.C. Uncollided Leakage and Flux on a Homogeneous Sphere

The total uncollided leakage from a homogeneous sphere is found using chord-length theory in Ref. 4 (the derivation of Ref. 4 is repeated in Ref. 10). Here we derive the total uncollided leakage using ray-tracing. The sphere has radius a, macroscopic cross section Σ, and source rate density q.

Start with Eq. (28) with $K = 1$. Its solution is Eq. (33) with $\varphi(r_{1-},\mathbf{\Omega}_d) = 0$:

$$\varphi(r,\mathbf{\Omega}_d) = \frac{q}{4\pi\Sigma}\left(1 - e^{-\Sigma(r-r_{1-})}\right). \tag{42}$$

The angular flux in direction $\mathbf{\Omega}_d$ at the detector location r_d, which is a point on the surface of the sphere, is

$$\varphi(r_d, \mathbf{\Omega}_d) = \frac{q}{4\pi\Sigma}\left(1 - e^{-\Sigma(r_d - r_{1-})}\right). \tag{43}$$

Clearly, the distance $r_d - r_{1-}$, the path length through the sphere along the ray $\mathbf{\Omega}_d$, depends on the angles θ and ω defining $\mathbf{\Omega}_d$ (see Fig. 1). For each ray $\mathbf{\Omega}_d$, we compute this distance in any convenient coordinate system. For spherical symmetry, we don't need the polar angle cosine ω. Let

$$\mu \equiv \mathbf{\Omega}_d \cdot \mathbf{n}, \tag{44}$$

where $\mathbf{n}$ is the outward unit normal from the sphere at the detector point. See Fig. 2, where $d \equiv r_d - r_{1-}$ and it is clear that

$$\mu = \frac{d/2}{a} \tag{45}$$

and therefore

$$d = 2a\mu. \tag{46}$$

Using Eq. (46), Eq. (43) becomes

$$\varphi(r_d, \mathbf{\Omega}_d) = \frac{q}{4\pi\Sigma}\left(1 - e^{-2\Sigma a\mu}\right). \tag{47}$$

The partial current density $J_+(r_d)$ at the detector point is the angular flux multiplied by the surface-crossing cosine and integrated over all exiting angles:[5]

$$\begin{aligned} J_+(r_d) &= \int_0^{2\pi} d\omega \int_0^1 d\mu\, \mu\, \varphi(r, \mathbf{\Omega}_d) \\ &= \frac{q}{4\pi\Sigma} \int_0^{2\pi} d\omega \int_0^1 d\mu\, \mu \left(1 - e^{-2\Sigma a\mu}\right) \\ &= \frac{q}{2\Sigma} \int_0^1 d\mu\, \mu \left(1 - e^{-2\Sigma a\mu}\right). \end{aligned} \tag{48}$$

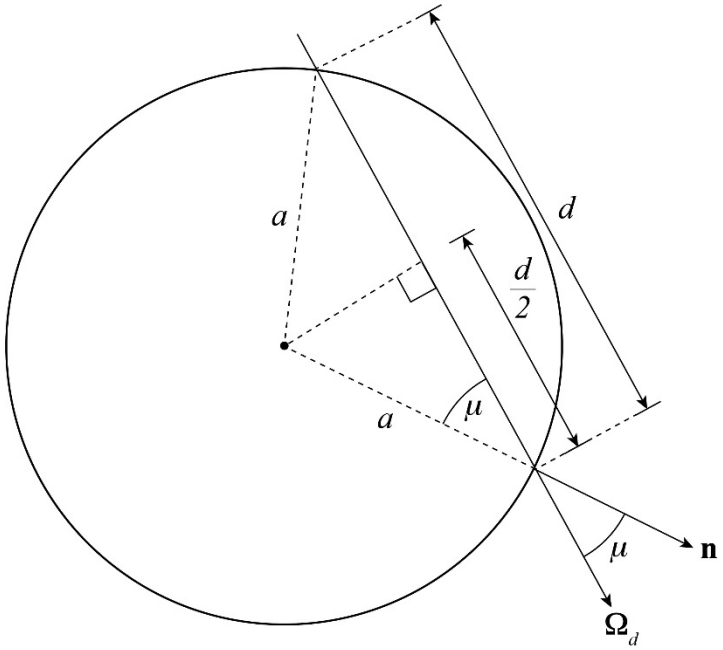

Figure 2. Ray-tracing in a homogeneous sphere.

Using the Wolfram on-line integrator[11] for the integral yields

$$\begin{aligned} J_+(r_d) &= \frac{q}{2\Sigma}\left\{\left[\frac{1}{2}\mu^2\right]_0^1 + \left[\frac{(1+2\Sigma a\mu)e^{-2\Sigma a\mu}}{(2\Sigma a)^2}\right]_0^1\right\} \\ &= \frac{q}{2\Sigma}\left\{\frac{1}{2} + \frac{(1+2\Sigma a)e^{-2\Sigma a}}{(2\Sigma a)^2} - \frac{1}{(2\Sigma a)^2}\right\} \\ &= \frac{1}{8a^2}\frac{q}{\Sigma}\left\{2a^2 - \frac{1}{\Sigma^2} + \frac{(1+2\Sigma a)e^{-2\Sigma a}}{\Sigma^2}\right\}. \end{aligned} \tag{49}$$

The total leakage L from the sphere is the integral of $J_+(r_d)$ [Eq. (49)] on the surface. Since $J_+(r_d)$ is a constant on the surface of the one-dimensional sphere, this integration amounts to multiplying Eq. (49) by the surface area of the sphere to obtain

$$\begin{aligned} L &= 4\pi a^2 J_+(r_d) \\ &= \frac{\pi}{2}\frac{q}{\Sigma}\left\{2a^2 - \frac{1}{\Sigma^2} + \frac{(1+2\Sigma a)e^{-2\Sigma a}}{\Sigma^2}\right\}, \end{aligned} \tag{50}$$

which is the same as Eq. (142) in Ref. 2.

Equation (142) in Ref. 2 can also be derived by ray-tracing the 1st-LASS adjoint flux [Eq. (41)]. The response function for the leakage, using $r = r_d = r_{1+}$ to designate a point on the surface, is $\Sigma_d(r_d, \mathbf{\Omega}_d) = |\mathbf{\Omega}_d \cdot \mathbf{n}|$. From Eqs. (39) and (40), the adjoint is

$$\psi^{(1)}(r, \mathbf{\Omega}_d) = e^{-\Sigma_{t,k}(r - r_d)}. \tag{51}$$

From Eq. (41), the partial current density at $r = r_d$ is

$$\begin{aligned} J_+(0) &= \int dV \int_{4\pi} d\mathbf{\Omega}\, \frac{q}{4\pi}\psi^{(1)}(r, \mathbf{\Omega}) \\ &= \int_{2\pi} d\mathbf{\Omega}_d\, |\mathbf{\Omega}_d \cdot \mathbf{n}| \int_{r_{1-}(\mathbf{\Omega})}^{r_d} dr\, \frac{q}{4\pi}\psi^{(1)}(r, \mathbf{\Omega}) \\ &= \frac{q}{2}\int_0^1 d\mu\, |\mu| \int_0^d dr\, e^{-\Sigma r} \\ &= \frac{q}{2}\int_0^1 d\mu\, \mu \frac{1}{\Sigma}\left(1 - e^{-\Sigma d}\right). \end{aligned} \tag{52}$$

Use Eq. (46) for d, evaluate the integral, and integrate over the surface of the sphere to obtain Eq. (50), which is the same as Eq. (142) in Ref. 2.

Chilton et al. derive the uncollided scalar flux at a point on the surface of a homogeneous sphere using the detector response at the center of a spherical surface source.[12] Here we do it using ray-tracing. Equation (47) gives the uncollided angular flux at a point on the surface (the detector point). The uncollided scalar flux at the detector point is, in akin with Eq. (48),

$$\begin{aligned}\phi(r_d) &= \int_0^{2\pi} d\omega \int_0^1 d\mu\, \varphi(r,\mathbf{\Omega}_d) \\ &= \frac{q}{4\pi\Sigma}\int_0^{2\pi} d\omega \int_0^1 d\mu \left(1-e^{-2\Sigma a\mu}\right) \\ &= \frac{q}{2\Sigma}\int_0^1 d\mu \left(1-e^{-2\Sigma a\mu}\right).\end{aligned} \tag{53}$$

Evaluating the integral yields

$$\phi(r_d) = \frac{q}{2\Sigma}\left[1-\frac{1}{2\Sigma a}\left(1-e^{-2\Sigma a}\right)\right], \tag{54}$$

which is Chilton et al.'s Eq. (6.99) when their $\hat{R} = 1/(4\pi)$. Equation (54) can also be derived using the uncollided 1st-LASS adjoint flux and Eq. (41).

III.D. 2nd LASS Forward Equation

Equations (8), (15), and (22) may be written

$$\mathbf{\Omega}\cdot\nabla\psi_1^{(2)}(\mathbf{r},\mathbf{\Omega}) + \Sigma_t(\mathbf{r})\psi_1^{(2)}(\mathbf{r},\mathbf{\Omega}) = -Q_{1,a}^{(2)}(\mathbf{r})\varphi(\mathbf{r},\mathbf{\Omega}) + Q_{1,b}^{(2)}(\mathbf{r}), \tag{55}$$

with boundary condition

$$\psi_1^{(2)}(\mathbf{r}_s,\mathbf{\Omega}) = 0,\ \mathbf{r}_s \in \partial V,\ \mathbf{\Omega}\cdot\mathbf{n} < 0. \tag{56}$$

We solve Eq. (55) along a particular ray from r_{max} to r_d in material region k (see Fig. 1). In this case, Eq. (55) becomes (for the subset of angles $\mathbf{\Omega}_d$)

$$\frac{\partial\psi_1^{(2)}(r,\mathbf{\Omega}_d)}{\partial r} + \Sigma_{t,k}\psi_1^{(2)}(r,\mathbf{\Omega}_d) = -Q_{1,a,k}^{(2)}\varphi(r,\mathbf{\Omega}_d) + Q_{1,b,k}^{(2)},\quad k = 1,\ldots,K, \tag{57}$$

where r is the distance along the ray in direction $\mathbf{\Omega}_d$. The 1st-LASS forward flux $\varphi(r,\mathbf{\Omega}_d)$ along the ray within region k is given by Eq. (33).

It is convenient to solve Eq. (57) separately for each source. For the first source on the right side (subscript a), using Eq. (33) in Eq. (57) and using the integrating factor $e^{\Sigma_{t,k}(r-r_{k-})}$ yields

$$\frac{\partial}{\partial r}\left(e^{\Sigma_{t,k}(r-r_{k-})}\psi_{1,a}^{(2)}(r,\mathbf{\Omega}_d)\right) = -Q_{1,a,k}^{(2)}\left\{\frac{q_k}{4\pi\Sigma_{t,k}}\left(e^{\Sigma_{t,k}(r-r_{k-})}-1\right) + \varphi(r_{k-},\mathbf{\Omega}_d)\right\}. \tag{58}$$

Clearly, the distance $r - r_{k-}$ depends on the angles θ and ω defining $\mathbf{\Omega}_d$ (see Fig. 1), so the functional dependence is suppressed. Integrating Eq. (58) yields

$$\begin{aligned}e^{\Sigma_{t,k}(r-r_{k-})}\psi_{1,a}^{(2)}(r,\mathbf{\Omega}_d) &= -Q_{1,a,k}^{(2)}\left\{\frac{q_k}{4\pi\Sigma_{t,k}}\int dr\,\left\{e^{\Sigma_{t,k}(r-r_{k-})}-1\right\} + \int dr\,\varphi(r_{k-},\mathbf{\Omega}_d)\right\} + C_a \\ &= -Q_{1,a,k}^{(2)}\left\{\frac{q_k}{4\pi\Sigma_{t,k}}\left(\frac{e^{\Sigma_{t,k}(r-r_{k-})}}{\Sigma_{t,k}} - (r-r_{k-})\right) + (r-r_{k-})\varphi(r_{k-},\mathbf{\Omega}_d)\right\} + C_a \\ &= -Q_{1,a,k}^{(2)}\left\{\frac{q_k}{4\pi\Sigma_{t,k}^2}e^{\Sigma_{t,k}(r-r_{k-})} - \left(\frac{q_k}{4\pi\Sigma_{t,k}} - \varphi(r_{k-},\mathbf{\Omega}_d)\right)(r-r_{k-})\right\} + C_a.\end{aligned} \tag{59}$$

Dividing through by the integrating factor yields

$$\psi_{1,a}^{(2)}(r,\mathbf{\Omega}_d) = -Q_{1,a,k}^{(2)}\left\{\frac{q_k}{4\pi\,\Sigma_{t,k}^2} - \left(\frac{q_k}{4\pi\,\Sigma_{t,k}} - \varphi(r_{k-},\mathbf{\Omega}_d)\right)(r-r_{k-})e^{-\Sigma_{t,k}(r-r_{k-})}\right\} + C_a e^{-\Sigma_{t,k}(r-r_{k-})}. \tag{60}$$

Designate the 2nd-LASS forward flux entering region *k* in direction $\mathbf{\Omega}_d$ as $\psi_{1,a}^{(2)}(r_{k-},\mathbf{\Omega}_d)$. Using $r = r_{k-}$ in Eq. (60) yields

$$\psi_{1,a}^{(2)}(r_{k-},\mathbf{\Omega}_d) = -Q_{1,a,k}^{(2)}\frac{q_k}{4\pi\,\Sigma_{t,k}^2} + C_a, \tag{61}$$

or

$$C_a = \psi_{1,a}^{(2)}(r_{k-},\mathbf{\Omega}_d) + Q_{1,a,k}^{(2)}\frac{q_k}{4\pi\,\Sigma_{t,k}^2}. \tag{62}$$

Using Eq. (62) in Eq. (60) yields

$$\begin{aligned}\psi_{1,a}^{(2)}(r,\mathbf{\Omega}_d) &= -Q_{1,a,k}^{(2)}\left\{\frac{q_k}{4\pi\,\Sigma_{t,k}^2} - \left(\frac{q_k}{4\pi\,\Sigma_{t,k}} - \varphi(r_{k-},\mathbf{\Omega}_d)\right)(r-r_{k-})e^{-\Sigma_{t,k}(r-r_{k-})}\right\} \\ &\quad + \left\{\psi_{1,a}^{(2)}(r_{k-},\mathbf{\Omega}_d) + Q_{1,a,k}^{(2)}\frac{q_k}{\Sigma_{t,k}^2}\right\}e^{-\Sigma_{t,k}(r-r_{k-})} \\ &= Q_{1,a,k}^{(2)}\left\{\frac{q_k}{4\pi\,\Sigma_{t,k}^2}\left(e^{-\Sigma_{t,k}(r-r_{k-})}-1\right) + \left(\frac{q_k}{4\pi\,\Sigma_{t,k}} - \varphi(r_{k-},\mathbf{\Omega}_d)\right)(r-r_{k-})e^{-\Sigma_{t,k}(r-r_{k-})}\right\} \\ &\quad + e^{-\Sigma_{t,k}(r-r_{k-})}\psi_{1,a}^{(2)}(r_{k-},\mathbf{\Omega}_d).\end{aligned} \tag{63}$$

The second source on the right side of Eq. (57) (subscript *b*) is a constant in region *k*. The solution can be written immediately by analogy with Eq. (33):

$$\psi_{1,b}^{(2)}(r,\mathbf{\Omega}_d) = Q_{1,b,k}^{(2)}\left\{\frac{1}{\Sigma_{t,k}}\left(1-e^{-\Sigma_{t,k}(r-r_{k-})}\right)\right\} + e^{-\Sigma_{t,k}(r-r_{k-})}\psi_{1,b}^{(2)}(r_{k-},\mathbf{\Omega}_d). \tag{64}$$

The boundary condition, given by applying Eq. (56) to Fig. 1, completes the solution for both $\psi_{1,a}^{(2)}(r,\mathbf{\Omega}_d)$ and $\psi_{1,b}^{(2)}(r,\mathbf{\Omega}_d)$:

$$\psi_1^{(2)}(r_{max},\mathbf{\Omega}_d) = 0. \tag{65}$$

III.E. Specific Solutions of 2nd-LASS Forward Equations

The equations of the 2nd-LASS include the same forward transport operator as Eq. (1) or the same adjoint transport operator as Eq. (3). Two of the forward equations [Eqs. (8) and (15)] have sources that include the 1st-LASS forward flux $\varphi(r,\mathbf{\Omega}_d)$. The solution of these equations in region *k* is Eq. (63) with

$$Q_{1,a}^{(2)} = \sigma_i f_i(\mathbf{r}) \tag{66}$$

for Eq. (8) and

$$Q_{1,a}^{(2)} = N_i f_i(\mathbf{r}) \tag{67}$$

for Eq. (15). Note that Eq. (63) already includes the negative sign preceding these sources in Eqs. (8) and (15).

Two of the forward equations [Eqs. (8) and (22)] have sources that include the source emission rate or atom density of isotope *i*, but not the 1st-LASS forward flux $\varphi(r,\mathbf{\Omega}_d)$. The solution of these equations in region *k* is Eq. (64) with

$$Q_{1,b}^{(2)} = q_i g_i(\mathbf{r}) \tag{68}$$

for Eq. (8) and

$$Q_{1,b}^{(2)} = N_i g_i(\mathbf{r}) \tag{69}$$

for Eq. (22).

The solution of Eq. (8) is the sum of Eqs. (63) and (64), using Eqs. (66) and (68):

$$\begin{aligned}\psi_{1,i}^{(2)}(r,\mathbf{\Omega}_d) = \sigma_i f_i(\mathbf{r})&\left\{\frac{q_k}{4\pi\,\Sigma_{t,k}^2}\left(e^{-\Sigma_{t,k}(r-r_{k-})}-1\right)+\left(\frac{q_k}{4\pi\,\Sigma_{t,k}}-\varphi(r_{k-},\mathbf{\Omega}_d)\right)(r-r_{k-})e^{-\Sigma_{t,k}(r-r_{k-})}\right\}\\ &+e^{-\Sigma_{t,k}(r-r_{k-})}\psi_{1,i,a}^{(2)}(r_{k-},\mathbf{\Omega}_d)\\ &+\frac{q_i g_i(\mathbf{r})}{4\pi\,\Sigma_{t,k}}\left(1-e^{-\Sigma_{t,k}(r-r_{k-})}\right)+e^{-\Sigma_{t,k}(r-r_{k-})}\psi_{1,i,b}^{(2)}(r_{k-},\mathbf{\Omega}_d).\end{aligned} \tag{70}$$

The solution of Eq. (15) is Eq. (63), using Eq. (67):

$$\begin{aligned}\psi_{1,i+N_m}^{(2)}(r,\mathbf{\Omega}_d) = N_i f_i(\mathbf{r})&\left\{\frac{q_k}{4\pi\,\Sigma_{t,k}^2}\left(e^{-\Sigma_{t,k}(r-r_{k-})}-1\right)+\left(\frac{q_k}{4\pi\,\Sigma_{t,k}}-\varphi(r_{k-},\mathbf{\Omega}_d)\right)(r-r_{k-})e^{-\Sigma_{t,k}(r-r_{k-})}\right\}\\ &+e^{-\Sigma_{t,k}(r-r_{k-})}\psi_{1,i+N_m}^{(2)}(r_{k-},\mathbf{\Omega}_d).\end{aligned} \tag{71}$$

The solution of Eq. (22) is Eq. (64), using Eq. (69):

$$\psi_{1,i+2N_m}^{(2)}(r,\mathbf{\Omega}_d) = \frac{N_i g_i(\mathbf{r})}{\Sigma_{t,k}}\left(1-e^{-\Sigma_{t,k}(r-r_{k-})}\right)+e^{-\Sigma_{t,k}(r-r_{k-})}\psi_{1,i+2N_m}^{(2)}(r_{k-},\mathbf{\Omega}_d). \tag{72}$$

Note the importance of retaining $\psi_{1,i,a}^{(2)}(r_{k-},\mathbf{\Omega}_d)$ and $\psi_{1,i,b}^{(2)}(r_{k-},\mathbf{\Omega}_d)$ in Eq. (70) and the unimportance of doing so in Eqs. (71) and (72).

III.F. 2nd LASS Adjoint Equation

Equations (10) and (17) may be written

$$-\mathbf{\Omega}\cdot\nabla\psi_2^{(2)}(\mathbf{r},\mathbf{\Omega})+\Sigma_t(\mathbf{r})\psi_2^{(2)}(\mathbf{r},\mathbf{\Omega}) = -Q_2^{(2)}(\mathbf{r})\psi^{(1)}(\mathbf{r},\mathbf{\Omega}), \tag{73}$$

with boundary condition

$$\psi_2^{(2)}(\mathbf{r}_s,\mathbf{\Omega}) = 0,\ \mathbf{r}_s\in\partial V,\ \mathbf{\Omega}\cdot\mathbf{n}>0. \tag{74}$$

We solve Eq. (73) along a particular ray from r_d to r_{max} in material region *k* (see Fig. 1). Also, we recognize that particles are traveling in the negative direction, though we solve Eq. (73) in the forward direction. In this case, Eq. (73) becomes (for the subset of angles $\mathbf{\Omega}_d$)

$$\frac{\partial\psi_2^{(2)}(r,\mathbf{\Omega}_d)}{\partial r}+\Sigma_{t,k}\psi_2^{(2)}(r,\mathbf{\Omega}_d) = -Q_{2,k}^{(2)}\psi^{(1)}(r,\mathbf{\Omega}_d),\quad k=1,\ldots,K, \tag{75}$$

where *r* is the distance along the ray in direction $-\mathbf{\Omega}_d$. The 1st-LASS adjoint flux $\psi^{(1)}(\mathbf{r},\mathbf{\Omega})$ along the ray within region *k* is Eq. (39).

Using Eq. (39) in Eq. (75) and using the integrating factor $e^{\Sigma_{t,k}(r-r_{k+})}$ yields

$$\frac{\partial}{\partial r}\left(e^{\Sigma_{t,k}(r-r_{k+})}\psi_2^{(2)}(r,\mathbf{\Omega}_d)\right)=-Q_{2,k}^{(2)}\psi^{(1)}(r_{k+},\mathbf{\Omega}_d). \tag{76}$$

Clearly, the distance $r-r_{k+}$ depends on the angles θ and ω defining $\mathbf{\Omega}_d$ (see Fig. 1), so the functional dependence is suppressed. Integrating Eq. (76) yields

$$\begin{aligned} e^{\Sigma_{t,k}(r-r_{k+})}\psi_2^{(2)}(r,\mathbf{\Omega}_d) &= -Q_{2,k}^{(2)}\psi^{(1)}(r_{k+},\mathbf{\Omega}_d)\int dr\ + C \\ &= -Q_{2,k}^{(2)}\psi^{(1)}(r_{k+},\mathbf{\Omega}_d)(r-r_{k+})+C. \end{aligned} \tag{77}$$

Dividing through by the integrating factor yields

$$\psi_2^{(2)}(r,\mathbf{\Omega}_d)=-Q_{2,k}^{(2)}\psi^{(1)}(r_{k+},\mathbf{\Omega}_d)(r-r_{k+})e^{-\Sigma_{t,k}(r-r_{k+})}+Ce^{-\Sigma_{t,k}(r-r_{k+})}. \tag{78}$$

Designate the 2nd-LASS adjoint flux entering region *k* in direction $-\mathbf{\Omega}_d$ as $\psi_2^{(2)}(r_{k+},\mathbf{\Omega}_d)$. Using $r=r_{k+}$ in Eq. (78) yields

$$\psi_2^{(2)}(r_{k+},\mathbf{\Omega}_d)=C. \tag{79}$$

Using Eq. (79) in Eq. (78) yields

$$\begin{aligned} \psi_2^{(2)}(r,\mathbf{\Omega}_d) = Q_{2,k}^{(2)}&\left\{-(r-r_{k+})e^{-\Sigma_{t,k}(r-r_{k+})}\psi^{(1)}(r_{k+},\mathbf{\Omega}_d)\right\} \\ &+e^{-\Sigma_{t,k}(r-r_{k+})}\psi_2^{(2)}(r_{k+},\mathbf{\Omega}_d). \end{aligned} \tag{80}$$

The boundary condition, given by applying Eq. (74) to Fig. 1, completes the solution:

$$\psi_2^{(2)}(r_{K+},\mathbf{\Omega}_d)=0. \tag{81}$$

III.G. Specific Solutions of 2nd-LASS Adjoint Equations

Two of the adjoint equations [Eqs. (10) and (17)] have sources that include the 1st-LASS adjoint flux. The solution of these equations in region *k* is Eq. (80) with

$$Q_2^{(2)}=\sigma_i f_i(\mathbf{r}) \tag{82}$$

for Eq. (10) and

$$Q_2^{(2)}=N_i f_i(\mathbf{r}) \tag{83}$$

for Eq. (17). Note that Eq. (80) already includes the negative sign preceding these sources in Eqs. (10) and (17).

The solution of Eq. (10) is Eq. (80), using Eq. (82):

$$\psi_{2,i}^{(2)}(r,\mathbf{\Omega}_d)=\sigma_i f_i(\mathbf{r})\left\{-(r-r_{k+})e^{-\Sigma_{t,k}(r-r_{k+})}\psi^{(1)}(r_{k+},\mathbf{\Omega}_d)\right\}+e^{-\Sigma_{t,k}(r-r_{k+})}\psi_{2,i}^{(2)}(r_{k+},\mathbf{\Omega}_d). \tag{84}$$

The solution of Eq. (17) is Eq. (80), using Eq. (83):

$$\psi_{2,i+N_m}^{(2)}(r,\mathbf{\Omega}_d)=N_i f_i(\mathbf{r})\left\{-(r-r_{k+})e^{-\Sigma_{t,k}(r-r_{k+})}\psi^{(1)}(r_{k+},\mathbf{\Omega}_d)\right\}+e^{-\Sigma_{t,k}(r-r_{k+})}\psi_{2,i+N_m}^{(2)}(r_{k+},\mathbf{\Omega}_d). \tag{85}$$

Recall that $\psi_{2,i+2N_m}^{(2)}(r,\mathbf{\Omega}_d)=0$ (Sec. IV.C of Ref. 2).

IV. Inner Products of the 2nd-LASS

The inner products are derived for ray-tracing of the 1st-LASS in Ref. 4. Figure 1 shows a ray with direction $\mathbf{\Omega}$ traversing an arbitrary geometry towards a detector located at r_d. As noted in Sec. III, the angles that intersect r_d are denoted $\mathbf{\Omega}_d$. The following sections derive the inner products of the 2nd-LASS.

IV.A. Inner Products of $\psi_2^{(2)}(r,\mathbf{\Omega})$

The second-order sensitivities require the volume and angle integral of $\psi_{2,i}^{(2)}(r,\mathbf{\Omega})$ and $\psi_{2,i+N_m}^{(2)}(r,\mathbf{\Omega})$ [Eqs. (12), (14), (19), and (21)]. Denote these as $\int dV \int_{4\pi} d\mathbf{\Omega}\, \psi_2^{(2)}(r,\mathbf{\Omega})$. They will be computed by ray-tracing in direction $\mathbf{\Omega}_d$ towards the detector point:

$$\int dV \int_{4\pi} d\mathbf{\Omega}\, \psi_2^{(2)}(r,\mathbf{\Omega}) = \int_{2\pi} d\mathbf{\Omega}_d \left|\mathbf{\Omega}_d \cdot \mathbf{n}\right| \int_{r_{1-}(\mathbf{\Omega})}^{r_d} dr\, \psi_2^{(2)}(r,\mathbf{\Omega}_d). \tag{86}$$

The integral over $\mathbf{\Omega}_d$ is only over outgoing angles. The 2nd-LASS adjoints are either nonzero only along rays in direction $\mathbf{\Omega}_d$, or they are zero everywhere; therefore, the arguments on the right side of Eq. (86) are $\mathbf{\Omega}_d$.

The integral is the sum over regions:

$$\begin{aligned}\int dV \int_{4\pi} d\mathbf{\Omega}\, \psi_2^{(2)}(r,\mathbf{\Omega}) &= \sum_{k=1}^{K} \int_{2\pi} d\mathbf{\Omega}_d \left|\mathbf{\Omega}_d \cdot \mathbf{n}\right| \int_{r_{k-}}^{r_{k+}} dr\, \psi_2^{(2)}(r,\mathbf{\Omega}_d) \\ &= \sum_{k=1}^{K} \int_{2\pi} d\mathbf{\Omega}_d \left|\mathbf{\Omega}_d \cdot \mathbf{n}\right| \int_{r_{k-}}^{r_{k+}} dr\, Q_{2,k}^{(2)} \\ &\times \left\{-(r_{k+}-r)e^{-\Sigma_{t,k}(r_{k+}-r)}\psi^{(1)}(r_{k+},\mathbf{\Omega}_d)\right\} \\ &+ \sum_{k=1}^{K} \int_{2\pi} d\mathbf{\Omega}_d \left|\mathbf{\Omega}_d \cdot \mathbf{n}\right| \int_{r_{k-}}^{r_{k+}} dr\, e^{-\Sigma_{t,k}(r_{k+}-r)}\psi_2^{(2)}(r_{k+},\mathbf{\Omega}_d),\end{aligned} \tag{87}$$

where $Q_{2,k}^{(2)}$ is Eq. (82) or (83) if isotope *i* is present in region *k* and 0 if it is not. Integrating in direction $\mathbf{\Omega}_d$ towards the detector point causes $r - r_{k+}$ in Eqs. (84) and (85) to change sign to $r_{k+} - r$. The first integral along the ray in Eq. (87) is

$$\int_{r_{k-}}^{r_{k+}} dr\, Q_{2,k}^{(2)} \left\{-(r_{k+}-r)e^{-\Sigma_{t,k}(r_{k+}-r)}\psi_2^{(1)}(r_{k+},\mathbf{\Omega}_d)\right\} = Q_{2,k}^{(2)} \frac{1-(1+\Sigma_{t,k}d_k)e^{-\Sigma_{t,k}d_k}}{\Sigma_{t,k}^2}\psi^{(1)}(r_{k+},\mathbf{\Omega}_d). \tag{88}$$

The second integral along the ray in Eq. (87) is

$$\int_{r_{k-}}^{r_{k+}} dr\, e^{-\Sigma_{t,k}(r_{k+}-r)}\psi_2^{(2)}(r_{k+},\mathbf{\Omega}_d) = \frac{1-e^{-\Sigma_{t,k}d_k}}{\Sigma_{t,k}}\psi_2^{(2)}(r_{k+},\mathbf{\Omega}_d). \tag{89}$$

Adding Eqs. (88) and (89), Eq. (87) becomes

$$\begin{aligned}\int_{V_k} dV \int_{4\pi} d\mathbf{\Omega}\, \psi_2^{(2)}(r,\mathbf{\Omega}) = \sum_{k=1}^{K} \int_{2\pi} d\mathbf{\Omega}_d \left|\mathbf{\Omega}_d \cdot \mathbf{n}\right| \Bigg\{ & Q_{2,k}^{(2)} \frac{1-(1+\Sigma_{t,k}d_k)e^{-\Sigma_{t,k}d_k}}{\Sigma_{t,k}^2}\psi^{(1)}(r_{k+},\mathbf{\Omega}_d) \\ & + \frac{1-e^{-\Sigma_{t,k}d_k}}{\Sigma_{t,k}}\psi_2^{(2)}(r_{k+},\mathbf{\Omega}_d)\Bigg\}.\end{aligned} \tag{90}$$

The remaining integral on the right side of Eq. (90) is evaluated using numerical quadrature.

IV.B. Inner Products of $\psi_1^{(2)}(r,\mathbf{\Omega})\times\psi^{(1)}(r,\mathbf{\Omega})$

The second-order sensitivities also require the volume and angle integral of $\psi_{1,i}^{(2)}(r,\mathbf{\Omega})\times\psi^{(1)}(r,\mathbf{\Omega})$, $\psi_{1,i+N_m}^{(2)}(r,\mathbf{\Omega})\times\psi^{(1)}(r,\mathbf{\Omega})$, and $\psi_{1,i+2N_m}^{(2)}(r,\mathbf{\Omega})\times\psi^{(1)}(r,\mathbf{\Omega})$ [Eqs. (12), (13), (19), (20), (24), and (25)]. These integrals have the same form. Because the 1st-LASS adjoint is only nonzero along $\mathbf{\Omega}_d$, these products are only nonzero along $\mathbf{\Omega}_d$, so these integrals are evaluated using ray-tracing. For the $\psi_{1,a}^{(2)}(r,\mathbf{\Omega}_d)$ component [Eq. (63)], ray-tracing in direction $\mathbf{\Omega}_d$ towards the detector point, it is

$$\begin{aligned}
&\int dV\int_{4\pi} d\mathbf{\Omega}\,\psi_{1,a}^{(2)}(r,\mathbf{\Omega})\times\psi^{(1)}(r,\mathbf{\Omega}) = \\
&\sum_{k=1}^{K}\int_{2\pi} d\mathbf{\Omega}_d\,\left|\mathbf{\Omega}_d\cdot\mathbf{n}\right|\int_{r_{k-}}^{r_{k+}} dr\,Q_{1,a,k}^{(2)}\left\{\frac{q_k}{4\pi\,\Sigma_{t,k}^2}\left(e^{-\Sigma_{t,k}(r-r_{k-})}-1\right)\right. \\
&\left.+\left(\frac{q_k}{4\pi\,\Sigma_{t,k}}-\varphi(r_{k-},\mathbf{\Omega}_d)\right)(r-r_{k-})e^{-\Sigma_{t,k}(r-r_{k-})}\right\}e^{-\Sigma_{t,k}(r_{k+}-r)}\psi^{(1)}(r_{k+},\mathbf{\Omega}_d) \\
&+\sum_{k=1}^{K}\int_{2\pi} d\mathbf{\Omega}_d\,\left|\mathbf{\Omega}_d\cdot\mathbf{n}\right|\int_{r_{k-}}^{r_{k+}} dr\,e^{-\Sigma_{t,k}(r-r_{k-})}\psi_{1,a}^{(2)}(r_{k-},\mathbf{\Omega}_d)e^{-\Sigma_{t,k}(r_{k+}-r)}\psi^{(1)}(r_{k+},\mathbf{\Omega}_d),
\end{aligned} \tag{91}$$

where $Q_{1,a,k}^{(2)}$ is Eq. (66) or (67) if isotope *i* is present in region *k* and 0 if it is not. Equation (91) reduces to

$$\begin{aligned}
&\int\ dV\int_{4\pi} d\mathbf{\Omega}\,\psi_{1,a}^{(2)}(r,\mathbf{\Omega})\times\psi^{(1)}(r,\mathbf{\Omega}) = \\
&\sum_{k=1}^{K}\int_{2\pi} d\mathbf{\Omega}_d\,\left|\mathbf{\Omega}_d\cdot\mathbf{n}\right|\int_{r_{k-}}^{r_{k+}} dr\,Q_{1,a,k}^{(2)}\,\frac{q_k}{4\pi\,\Sigma_{t,k}^2}\left(e^{-\Sigma_{t,k}d_k}-e^{-\Sigma_{t,k}(r_{k+}-r)}\right)\psi^{(1)}(r_{k+},\mathbf{\Omega}_d) \\
&+\sum_{k=1}^{K}\int_{2\pi} d\mathbf{\Omega}_d\,\left|\mathbf{\Omega}_d\cdot\mathbf{n}\right|\int_{r_{k-}}^{r_{k+}} dr\,Q_{1,a,k}^{(2)}\left(\frac{q_k}{4\pi\,\Sigma_{t,k}}-\varphi(r_{k-},\mathbf{\Omega}_d)\right)(r-r_{k-})e^{-\Sigma_{t,k}d_k}\psi^{(1)}(r_{k+},\mathbf{\Omega}_d) \\
&+\sum_{k=1}^{K}\int_{2\pi} d\mathbf{\Omega}_d\,\left|\mathbf{\Omega}_d\cdot\mathbf{n}\right|\int_{r_{k-}}^{r_{k+}} dr\,e^{-\Sigma_{t,k}d_k}\psi_{1,a}^{(2)}(r_{k-},\mathbf{\Omega}_d)\psi^{(1)}(r_{k+},\mathbf{\Omega}_d).
\end{aligned} \tag{92}$$

The first integral along the ray in Eq. (92) is

$$\begin{aligned}
&\int_{r_{k-}}^{r_{k+}} dr\,Q_{1,a,k}^{(2)}\,\frac{q_k}{4\pi\,\Sigma_{t,k}^2}\left(e^{-\Sigma_{t,k}d_k}-e^{-\Sigma_{t,k}(r_{k+}-r)}\right)\psi^{(1)}(r_{k+},\mathbf{\Omega}_d) = \\
&Q_{1,a,k}^{(2)}\,\frac{q_k}{4\pi\,\Sigma_{t,k}^2}\left(d_k e^{-\Sigma_{t,k}d_k}-\frac{1-e^{-\Sigma_{t,k}d_k}}{\Sigma_{t,k}}\right)\psi^{(1)}(r_{k+},\mathbf{\Omega}_d).
\end{aligned} \tag{93}$$

The second integral along the ray in Eq. (92) is

$$\begin{aligned}
&\int_{r_{k-}}^{r_{k+}} dr\,Q_{1,a,k}^{(2)}\left(\frac{q_k}{4\pi\,\Sigma_{t,k}}-\varphi(r_{k-},\mathbf{\Omega}_d)\right)(r-r_{k-})e^{-\Sigma_{t,k}d_k}\psi^{(1)}(r_{k+},\mathbf{\Omega}_d) = \\
&Q_{1,a,k}^{(2)}\left(\frac{q_k}{4\pi\,\Sigma_{t,k}}-\varphi(r_{k-},\mathbf{\Omega}_d)\right)\frac{1}{2}d_k^2 e^{-\Sigma_{t,k}d_k}\psi^{(1)}(r_{k+},\mathbf{\Omega}_d).
\end{aligned} \tag{94}$$

The third integral along the ray in Eq. (92) is the integrand times d_k. Adding these and rearranging, Eq. (91) becomes

$$\int dV \int_{4\pi} d\mathbf{\Omega}\, \psi_{1,a}^{(2)}(r,\mathbf{\Omega}) \times \psi^{(1)}(r,\mathbf{\Omega}) = \sum_{k=1}^{K} \int_{2\pi} d\mathbf{\Omega}_d \left|\mathbf{\Omega}_d \cdot \mathbf{n}\right| \left\{ -Q_{1,a,k}^{(2)} \frac{q_k}{4\pi \Sigma_{t,k}^3} \left[1 - \left(1 + \Sigma_{t,k} d_k\right) e^{-\Sigma_{t,k} d_k} \right] \right.$$
$$\left. + Q_{1,a,k}^{(2)} \frac{1}{2} \left(\frac{q_k}{4\pi \Sigma_{t,k}} - \varphi(r_{k-}, \mathbf{\Omega}_d) \right) d_k^2 e^{-\Sigma_{t,k} d_k} + d_k e^{-\Sigma_{t,k} d_k} \psi_{1,a}^{(2)}(r_{k-}, \mathbf{\Omega}_d) \right\} \psi^{(1)}(r_{k+}, \mathbf{\Omega}_d). \tag{95}$$

For the $\psi_{1,b}^{(2)}(r,\mathbf{\Omega}_d)$ component [Eq. (64)], the integral is

$$\int dV \int_{4\pi} d\mathbf{\Omega}\, \psi_{1,b}^{(2)}(r,\mathbf{\Omega}) \times \psi^{(1)}(r,\mathbf{\Omega}) =$$
$$\sum_{k=1}^{K} \int_{2\pi} d\mathbf{\Omega}_d \left|\mathbf{\Omega}_d \cdot \mathbf{n}\right| \int_{r_{k-}}^{r_{k+}} dr\, Q_{1,b,k}^{(2)} \frac{1}{\Sigma_{t,k}} \left(1 - e^{-\Sigma_{t,k}(r - r_{k-})}\right) e^{-\Sigma_{t,k}(r_{k+} - r)} \psi^{(1)}(r_{k+}, \mathbf{\Omega}_d) \tag{96}$$
$$+ \sum_{k=1}^{K} \int_{2\pi} d\mathbf{\Omega}_d \left|\mathbf{\Omega}_d \cdot \mathbf{n}\right| \int_{r_{k-}}^{r_{k+}} dr\, e^{-\Sigma_{t,k}(r - r_{k-})} \psi_{1,b}^{(2)}(r_{k-}, \mathbf{\Omega}_d) e^{-\Sigma_{t,k}(r_{k+} - r)} \psi^{(1)}(r_{k+}, \mathbf{\Omega}_d).$$

Equation (96) reduces to

$$\int dV \int_{4\pi} d\mathbf{\Omega}\, \psi_{1,b}^{(2)}(r,\mathbf{\Omega}) \times \psi^{(1)}(r,\mathbf{\Omega}) =$$
$$\sum_{k=1}^{K} \int_{2\pi} d\mathbf{\Omega}_d \left|\mathbf{\Omega}_d \cdot \mathbf{n}\right| \int_{r_{k-}}^{r_{k+}} dr\, Q_{1,b,k}^{(2)} \frac{1}{\Sigma_{t,k}} \left(e^{-\Sigma_{t,k}(r_{k+} - r)} - e^{-\Sigma_{t,k} d_k}\right) \psi^{(1)}(r_{k+}, \mathbf{\Omega}_d) \tag{97}$$
$$+ \sum_{k=1}^{K} \int_{2\pi} d\mathbf{\Omega}_d \left|\mathbf{\Omega}_d \cdot \mathbf{n}\right| \int_{r_{k-}}^{r_{k+}} dr\, e^{-\Sigma_{t,k} d_k} \psi_{1,b}^{(2)}(r_{k-}, \mathbf{\Omega}_d) \psi^{(1)}(r_{k+}, \mathbf{\Omega}_d).$$

The first integral along the ray in Eq. (97) is

$$\int_{r_{k-}}^{r_{k+}} dr\, Q_{1,b,k}^{(2)} \frac{1}{\Sigma_{t,k}} \left(e^{-\Sigma_{t,k}(r_{k+} - r)} - e^{-\Sigma_{t,k} d_k}\right) \psi^{(1)}(r_{k+}, \mathbf{\Omega}_d) = Q_{1,b,k}^{(2)} \frac{1}{\Sigma_{t,k}} \left(\frac{1 - e^{-\Sigma_{t,k} d_k}}{\Sigma_{t,k}} - d_k e^{-\Sigma_{t,k} d_k} \right) \psi^{(1)}(r_{k+}, \mathbf{\Omega}_d). \tag{98}$$

The second integral along the ray in Eq. (97) is the integrand times d_k. Adding these and rearranging, Eq. (96) becomes

$$\int dV \int_{4\pi} d\mathbf{\Omega}\, \psi_{1,b}^{(2)}(r,\mathbf{\Omega}) \times \psi^{(1)}(r,\mathbf{\Omega}) = \sum_{k=1}^{K} \int_{2\pi} d\mathbf{\Omega}_d \left|\mathbf{\Omega}_d \cdot \mathbf{n}\right| \left\{ Q_{1,b,k}^{(2)} \frac{1}{\Sigma_{t,k}^2} \left[1 - \left(1 + \Sigma_{t,k} d_k\right) e^{-\Sigma_{t,k} d_k} \right] \right.$$
$$\left. + d_k e^{-\Sigma_{t,k} d_k} \psi_{1,b}^{(2)}(r_{k-}, \mathbf{\Omega}_d) \right\} \psi^{(1)}(r_{k+}, \mathbf{\Omega}_d). \tag{99}$$

The remaining integrals on the right sides of Eqs. (95) and (99) are evaluated using numerical quadrature.

IV.C. Inner Products of $\psi_2^{(2)}(r,\mathbf{\Omega}) \times \varphi(r,\mathbf{\Omega})$

Finally, the second-order sensitivities also require the volume and angle integral of $\psi_{2,i}^{(2)}(r,\mathbf{\Omega}) \times \varphi(r,\mathbf{\Omega})$ and $\psi_{2,i+N_m}^{(2)}(r,\mathbf{\Omega}) \times \varphi(r,\mathbf{\Omega})$ [Eqs. (12), (13), (19), and (20)]. These integrals have the same form. Because the 2nd-LASS adjoint is only nonzero along $\mathbf{\Omega}_d$, these products are only nonzero along $\mathbf{\Omega}_d$, so these integrals are evaluated using ray-tracing. The integral is

$$\int dV \int_{4\pi} d\mathbf{\Omega}\, \psi_2^{(2)}(r,\mathbf{\Omega})\varphi(r,\mathbf{\Omega}) =$$

$$\sum_{k=1}^{K} \int_{2\pi} d\mathbf{\Omega}_d \left|\mathbf{\Omega}_d \cdot \mathbf{n}\right| \int_{r_{k-}}^{r_{k+}} dr\, Q_{2,k}^{(2)} \left\{-(r_{k+}-r) e^{-\Sigma_{t,k}(r_{k+}-r)} \psi^{(1)}(r_{k+},\mathbf{\Omega}_d)\right\} \frac{q_k}{4\pi\Sigma_{t,k}} \left(1-e^{-\Sigma_{t,k}(r-r_{k-})}\right)$$

$$+\sum_{k=1}^{K} \int_{2\pi} d\mathbf{\Omega}_d \left|\mathbf{\Omega}_d \cdot \mathbf{n}\right| \int_{r_{k-}}^{r_{k+}} dr\, e^{-\Sigma_{t,k}(r_{k+}-r)} \psi_2^{(2)}(r_{k+},\mathbf{\Omega}_d) \frac{q_k}{4\pi\Sigma_{t,k}} \left(1-e^{-\Sigma_{t,k}(r-r_{k-})}\right) \tag{100}$$

$$+\sum_{k=1}^{K} \int_{2\pi} d\mathbf{\Omega}_d \left|\mathbf{\Omega}_d \cdot \mathbf{n}\right| \int_{r_{k-}}^{r_{k+}} dr\, Q_{2,k}^{(2)} \left\{-(r_{k+}-r) e^{-\Sigma_{t,k}(r_{k+}-r)} \psi^{(1)}(r_{k+},\mathbf{\Omega}_d)\right\} \varphi(r_{k-},\Omega_d)\, e^{-\Sigma_{t,k}(r-r_{k-})}$$

$$+\sum_{k=1}^{K} \int_{2\pi} d\mathbf{\Omega}_d \left|\mathbf{\Omega}_d \cdot \mathbf{n}\right| \int_{r_{k-}}^{r_{k+}} dr\, e^{-\Sigma_{t,k}(r_{k+}-r)} \psi_2^{(2)}(r_{k+},\mathbf{\Omega}_d) \varphi(r_{k-},\Omega_d)\, e^{-\Sigma_{t,k}(r-r_{k-})},$$

where $Q_{2,k}^{(2)}$ is Eq. (82) or (83) if isotope *i* is present in region *k* and 0 if it is not. Equation (100) reduces to

$$\int dV \int_{4\pi} d\mathbf{\Omega}\, \psi_2^{(2)}(r,\mathbf{\Omega})\varphi(r,\mathbf{\Omega}) =$$

$$\sum_{k=1}^{K} \int_{2\pi} d\mathbf{\Omega}_d \left|\mathbf{\Omega}_d \cdot \mathbf{n}\right| \int_{r_{k-}}^{r_{k+}} dr\, Q_{2,k}^{(2)} \frac{q_k}{4\pi\Sigma_{t,k}} \left\{-(r_{k+}-r) e^{-\Sigma_{t,k}(r_{k+}-r)} \psi^{(1)}(r_{k+},\mathbf{\Omega}_d)\right\}$$

$$+\sum_{k=1}^{K} \int_{2\pi} d\mathbf{\Omega}_d \left|\mathbf{\Omega}_d \cdot \mathbf{n}\right| \int_{r_{k-}}^{r_{k+}} dr \frac{q_k}{4\pi\Sigma_{t,k}} e^{-\Sigma_{t,k}(r_{k+}-r)} \psi_2^{(2)}(r_{k+},\mathbf{\Omega}_d) \tag{101}$$

$$+\sum_{k=1}^{K} \int_{2\pi} d\mathbf{\Omega}_d \left|\mathbf{\Omega}_d \cdot \mathbf{n}\right| \int_{r_{k-}}^{r_{k+}} dr\, Q_{2,k}^{(2)} \left(\varphi(r_{k-},\Omega_d) - \frac{q_k}{4\pi\Sigma_{t,k}}\right) \left\{-(r_{k+}-r) e^{-\Sigma_{t,k}d_k} \psi^{(1)}(r_{k+},\mathbf{\Omega}_d)\right\}$$

$$+\sum_{k=1}^{K} \int_{2\pi} d\mathbf{\Omega}_d \left|\mathbf{\Omega}_d \cdot \mathbf{n}\right| \int_{r_{k-}}^{r_{k+}} dr \left(\varphi(r_{k-},\Omega_d) - \frac{q_k}{4\pi\Sigma_{t,k}}\right) e^{-\Sigma_{t,k}d_k} \psi_2^{(2)}(r_{k+},\mathbf{\Omega}_d).$$

The first integral along the ray in Eq. (101) is

$$\int_{r_{k-}}^{r_{k+}} dr\, Q_{2,k}^{(2)} \frac{q_k}{4\pi\Sigma_{t,k}} \left\{-(r_{k+}-r) e^{-\Sigma_{t,k}(r_{k+}-r)} \psi^{(1)}(r_{k+},\mathbf{\Omega}_d)\right\} = Q_{2,k}^{(2)} \frac{q_k}{4\pi\Sigma_{t,k}} \frac{1-(\Sigma_{t,k}d_k+1)e^{-\Sigma_{t,k}d_k}}{\Sigma_{t,k}^2}. \tag{102}$$

The second integral along the ray in Eq. (101) is

$$\int_{r_{k-}}^{r_{k+}} dr \frac{q_k}{4\pi\Sigma_{t,k}} e^{-\Sigma_{t,k}(r_{k+}-r)} \psi_2^{(2)}(r_{k+},\mathbf{\Omega}_d) = \frac{q_k}{4\pi\Sigma_{t,k}} \psi_2^{(2)}(r_{k+},\mathbf{\Omega}_d) \frac{1-e^{-\Sigma_{t,k}d_k}}{\Sigma_{t,k}}. \tag{103}$$

The third integral along the ray in Eq. (101) is

$$\int_{r_{k-}}^{r_{k+}} dr\, Q_{2,k}^{(2)} \left(\varphi(r_{k-},\Omega_d) - \frac{q_k}{4\pi\Sigma_{t,k}}\right) \left\{-(r_{k+}-r) e^{-\Sigma_{t,k}d_k} \psi^{(1)}(r_{k+},\mathbf{\Omega}_d)\right\} =$$

$$-\frac{1}{2} Q_{2,k}^{(2)} \left(\varphi(r_{k-},\Omega_d) - \frac{q_k}{4\pi\Sigma_{t,k}}\right) d_k^2 e^{-\Sigma_{t,k}d_k} \psi^{(1)}(r_{k+},\mathbf{\Omega}_d) \tag{104}$$

The fourth integral along the ray in Eq. (101) is the integrand times d_k. Adding these and rearranging, Eq. (101) becomes

$$\int dV \int_{4\pi} d\mathbf{\Omega}\, \psi_2^{(2)}(r,\mathbf{\Omega})\varphi(r,\mathbf{\Omega}) =$$
$$\sum_{k=1}^{K} \int_{2\pi} d\mathbf{\Omega}_d \left|\mathbf{\Omega}_d \cdot \mathbf{n}\right| \left\{ Q_{2,k}^{(2)} \frac{q_k}{4\pi \Sigma_{t,k}^3} \left[1 - (\Sigma_{t,k} d_k + 1) e^{-\Sigma_{t,k} d_k} \right] \right.$$
$$+ \frac{1}{2} Q_{2,k}^{(2)} \left(\frac{q_k}{4\pi \Sigma_{t,k}} - \varphi(r_{k-}, \Omega_d) \right) d_k^2 e^{-\Sigma_{t,k} d_k} \psi^{(1)}(r_{k+}, \mathbf{\Omega}_d) \qquad (105)$$
$$\left. + \left[\frac{q_k}{4\pi \Sigma_{t,k}^2} \left(1 - e^{-\Sigma_{t,k} d_k} \right) + \left(\varphi(r_{k-}, \Omega_d) - \frac{q_k}{4\pi \Sigma_{t,k}} \right) d_k e^{-\Sigma_{t,k} d_k} \right] \psi_2^{(2)}(r_{k+}, \mathbf{\Omega}_d) \right\}.$$

The remaining integral on the right side of Eq. (105) is evaluated using numerical quadrature.

V. Numerical Results for an Analytic Sphere

The equations of Sec. IV were implemented in the SENSPG computer code, and the integrals were evaluated using the QUADPACK integration library.[13] The homogeneous sphere with two isotopes that was described in Ref. 2 and solved there using PARTISN was solved using ray-tracing. The SENSPG input file is listed in the appendix.

Material density derivatives are obtained from the isotopic density results using the chain rule:

$$\frac{\partial L}{\partial \rho} = \sum_{i=1}^{2} \frac{\partial L}{\partial N_i} \frac{\partial N_i}{\partial \rho}$$
$$= \frac{N_1}{\rho} \frac{\partial L}{\partial N_1} + \frac{N_2}{\rho} \frac{\partial L}{\partial N_2}, \qquad (106)$$
$$\frac{\partial^2 L}{\partial \rho^2} = \sum_{i=1}^{2} \sum_{j=1}^{2} \frac{\partial^2 L}{\partial N_i \partial N_j} \frac{\partial N_i}{\partial \rho} \frac{\partial N_j}{\partial \rho}$$
$$= \left(\frac{N_1}{\rho} \right)^2 \frac{\partial^2 L}{\partial N_1^2} + 2 \frac{N_1}{\rho} \frac{N_2}{\rho} \frac{\partial^2 L}{\partial N_1 \partial N_2} + \left(\frac{N_2}{\rho} \right)^2 \frac{\partial^2 L}{\partial N_2^2}, \qquad (107)$$

as in the PARTISN results of Sec. VII.E of Ref. 2. These density derivatives are constant-volume partial derivatives.[7] Mixed derivatives involving the mass density are obtained similarly.

All of the ray-trace inner products are identical to the analytic derivatives of Sec. VII.C of Ref. 2 to the number of digits shown there, except that $\partial^2 L/\partial\rho\partial\sigma_2$ and $\partial^2 L/\partial\rho\partial q_1$ each differ in the last digit from the values shown in Table VII of Ref. 2.

Reference 2 did not consider the sensitivity of the leakage to interface locations. Preparing for future work, we will do so here. The derivative of the total leakage with respect to the radius of the sphere, a, is

$$\frac{\partial L}{\partial a} = \frac{2\pi q_1 N_1 a}{\Sigma} \left(1 - e^{-2\Sigma a} \right), \qquad (108)$$

where q_1 and N_1 are the emission rate of the gamma-ray line from isotope 1 and the atom density of isotope 1, respectively. Using the parameters for the sphere given in Ref. 2, Eq. (108) evaluates to 5.700528×10^4 γ/s/cm. The adjoint-based formula, Eq. (39) of Ref. 14, when evaluated using ray-tracing,[6] yields the same result.

VI. Numerical Results for a Two-Region Slab

In preparation for an analytic benchmark, a two-region slab problem was done using ray-tracing. The slab is shown in Figure 3. The left region, with a thickness $t_1 = 4$ cm, represents uranium metal enriched to 20 wt% ^{235}U. Its density is 18.8 g/cm^3. The right region, with a thickness $t_2 = 6$ cm, represents natural uranium dioxide, UO_2, at a density of 10 g/cm^3. The quantity of interest is the leakage (partial current density) of the 1.001-MeV ^{238}U line from the right side of the slab. Parameters of the slab are given in Table I. Microscopic photon cross sections at 1.001 MeV and the 1.001-MeV line emission rate are given in Table II. The cross sections were obtained from the MCPLIB04 ACE-formatted photon cross-section library, which is distributed with MCNP, and do not contain coherent scattering. The source emission rate is from Gunnick.[15] The total macroscopic cross sections Σ_1 and Σ_2 and the total source rate densities Q_1 and Q_2 shown on Table I are computed using the data of Table II. The isotopic number densities are given in Table III. The SENSPG input file is listed in the appendix.

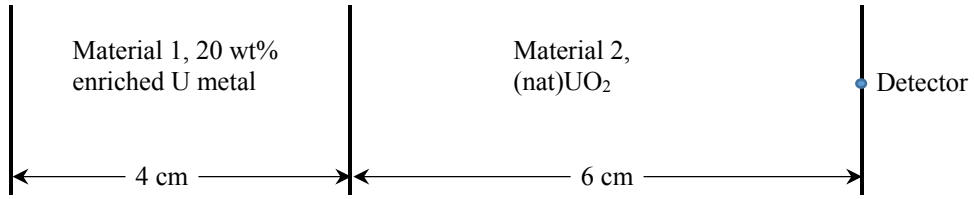

Figure 3. Two-region slab.

Table I. Slab Material Parameters.

Parameter	Value
Material 1	^{235}U, 20 wt%; ^{238}U, 80 wt%
ρ_1	18.8 g/cm^3
Σ_1	1.415651053 /cm
Q_1	6.137765449×10^3 γ/cm^3/s
t_1	4 cm
Material 2	^{235}U, 0.6267397832 wt%; ^{238}U, 87.52600761 wt%; ^{16}O, 11.84725261 wt%
ρ_2	10 g/cm^3
Σ_2	0.7374702915 /cm
Q_2	5.357853445×10^3 γ/cm^3/s
t_2	6 cm
L	302.60662 γ/s

Table II. Isotope Parameters.

Isotope	Cross section, σ (b)	Source emission rate, q [γ/(10^{24} atoms)/s]
^{235}U	29.69028616189	0.
^{238}U	29.69028616189	4.033×10^4
^{16}O	1.688362446543	0.

Table III. Isotope Densities.

Material	Isotope	Density (atom/b·cm)
1	^{235}U	$9.633468185116 \times 10^{-3}$
	^{238}U	$3.804714511001 \times 10^{-2}$
2	^{235}U	$1.605765362130 \times 10^{-4}$
	^{238}U	$2.214172016178 \times 10^{-2}$
	^{16}O	$4.460459339467 \times 10^{-2}$

First-order sensitivities are presented in Tables IV and V. Second-order sensitivities are presented in Tables VI through IX. These sensitivities compare very well with those computed using PARTISN with S_{2048} quadrature. Only a few differences are greater than 0.002% (in magnitude) and none are greater than 0.03% (in magnitude). Units of the sensitivities are suppressed; they correspond to those used in Tables I through III.

Table IV. First-Order Sensitivities (Absolute) of the Leakage to Isotopic Parameters.

Isotope	N	σ	q
^{235}U (mat. 1)	–1.89732E+01[(a)]	–6.15615E-03	0.00000E+00
^{238}U (mat. 1)	5.08497E+00	–2.43136E-02	2.26964E-05
^{235}U (mat. 2)	–1.21237E+04	–6.55696E-02	0.00000E+00
^{238}U (mat. 2)	1.50178E+03	–9.04132E+00	7.48057E-03
^{16}O	–6.89423E+02	–1.82138E+01	0.00000E+00

(a) For example, this number is the derivative of the leakage with respect to the ^{235}U number density in material 1.

Table V. First-Order Sensitivities (Absolute) of the Leakage to Densities and Surface Locations.

Parameter	Sensitivity
ρ_1	5.68661E-04
ρ_2	5.53732E-02
r_0	–2.67271E-03
r_1	–8.96160E-02
r_2	9.22887E-02

Table VI. Second-Order Sensitivities (Absolute) of the Leakage to Atom Densities and Isotopic Parameters.

Parameter	Isotope	*N*	*σ*	*q*
^{235}U *N* (mat. 1)	^{235}U (mat. 1)	7.66964E+02	–3.90185E-01	0.00000E+00
	^{238}U (mat. 1)	2.68287E+02	9.82839E-01	–4.70449E-04
	^{235}U (mat. 2)	3.88136E+03	2.09919E-02	0.00000E+00
	^{238}U (mat. 2)	3.88136E+03	2.89455E+00	0.00000E+00
	^{16}O	2.20717E+02	5.83108E+00[(a)]	0.00000E+00
^{238}U *N* (mat. 1)	^{235}U (mat. 1)	2.68287E+02	8.70499E-02	0.00000E+00
	^{238}U (mat. 1)	–2.30390E+02	–2.95237E-01	1.26084E-04
	^{235}U (mat. 2)	–1.03705E+03	–5.60874E-03	0.00000E+00
	^{238}U (mat. 2)	–1.03705E+03	–7.73384E-01	0.00000E+00
	^{16}O	–5.89725E+01	–1.55798E+00	0.00000E+00
^{235}U *N* (mat. 2)	^{235}U (mat. 1)	3.88136E+03	1.25937E+00	0.00000E+00
	^{238}U (mat. 1)	–1.03705E+03	4.97383E+00	–4.64000E-03
	^{235}U (mat. 2)	9.56490E+05	–4.03166E+02	0.00000E+00
	^{238}U (mat. 2)	4.17392E+05	7.13308E+02	–2.95972E-01
	^{16}O	5.43916E+04	1.43696E+03	0.00000E+00
^{238}U *N* (mat. 2)	^{235}U (mat. 1)	3.88136E+03	1.25937E+00	0.00000E+00
	^{238}U (mat. 1)	–1.03705E+03	4.97383E+00	–4.64000E-03
	^{235}U (mat. 2)	4.17392E+05	2.25742E+00	0.00000E+00
	^{238}U (mat. 2)	–1.21706E+05	–9.70660E+01	4.18773E-02
	^{16}O	2.37353E+04	6.27060E+02	0.00000E+00
^{16}O *N*	^{235}U (mat. 1)	2.20717E+02	7.16148E-02	0.00000E+00
	^{238}U (mat. 1)	–5.89725E+01	2.82841E-01	–2.63857E-04
	^{235}U (mat. 2)	5.43916E+04	2.94171E-01	0.00000E+00
	^{238}U (mat. 2)	2.37353E+04	4.05629E+01	–1.68307E-02
	^{16}O	3.09302E+03	–3.26625E+02	0.00000E+00

(a) For example, this number is the second derivative of the leakage with respect to the ^{235}U number density in material 1 and the ^{16}O cross section.

Table VII. Second-Order Sensitivities (Absolute) of the Leakage to Microscopic Cross Sections and Isotopic Parameters.

Parameter	Isotope	N	σ	q
^{235}U σ (mat. 1)	^{235}U (mat. 1)	–3.90185E-01	8.07442E-05	0.00000E+00
	^{238}U (mat. 1)	8.70499E-02	3.18897E-04	–1.52645E-07[(a)]
	^{235}U (mat. 2)	1.25937E+00	6.81113E-06	0.00000E+00
	^{238}U (mat. 2)	1.25937E+00	9.39180E-04	0.00000E+00
	^{16}O	7.16148E-02	1.89198E-03	0.00000E+00
^{238}U σ (mat. 1)	^{235}U (mat. 1)	9.82839E-01	3.18897E-04	0.00000E+00
	^{238}U (mat. 1)	–2.95237E-01	1.25948E-03	–6.02866E-07
	^{235}U (mat. 2)	4.97383E+00	2.69004E-05	0.00000E+00
	^{238}U (mat. 2)	4.97383E+00	3.70927E-03	0.00000E+00
	^{16}O	2.82841E-01	7.47234E-03	0.00000E+00
^{235}U σ (mat. 2)	^{235}U (mat. 1)	2.09919E-02	6.81113E-06	0.00000E+00
	^{238}U (mat. 1)	–5.60874E-03	2.69004E-05	–2.50949E-08
	^{235}U (mat. 2)	–4.03166E+02	2.79779E-05	0.00000E+00
	^{238}U (mat. 2)	2.25742E+00	3.85785E-03	–1.60073E-06
	^{16}O	2.94171E-01	7.77165E-03	0.00000E+00
^{238}U σ (mat. 2)	^{235}U (mat. 1)	2.89455E+00	9.39180E-04	0.00000E+00
	^{238}U (mat. 1)	–7.73384E-01	3.70927E-03	–3.46031E-06
	^{235}U (mat. 2)	7.13308E+02	3.85785E-03	0.00000E+00
	^{238}U (mat. 2)	–9.70660E+01	5.31954E-01	–2.20723E-04
	^{16}O	4.05629E+01	1.07162E+00	0.00000E+00
^{16}O σ	^{235}U (mat. 1)	5.83108E+00	1.89198E-03	0.00000E+00
	^{238}U (mat. 1)	–1.55798E+00	7.47234E-03	–6.97081E-06
	^{235}U (mat. 2)	1.43696E+03	7.77165E-03	0.00000E+00
	^{238}U (mat. 2)	6.27060E+02	1.07162E+00	–4.44648E-04
	^{16}O	–3.26625E+02	2.15879E+00	0.00000E+00

(a) For example, this number is the second derivative of the leakage with respect to the ^{235}U cross section in material 1 and the ^{238}U source emission rate for the 1.001-MeV line.

Table VIII. Second-Order Sensitivities (Absolute) of the Leakage to Source Emission Rates and Isotopic Parameters.

Parameter	Isotope	N	σ	q
^{238}U q (mat. 1)	^{235}U (mat. 1)	–4.70449E-04	–1.52645E-07[(a)]	0.00000E+00
	^{238}U (mat. 1)	1.26084E-04	–6.02866E-07	0.00000E+00
	^{235}U (mat. 2)	–4.64000E-03	–2.50949E-08	0.00000E+00
	^{238}U (mat. 2)	–4.64000E-03	–3.46031E-06	0.00000E+00
	^{16}O	–2.63857E-04	–6.97081E-06	0.00000E+00
^{238}U q (mat. 2)	^{235}U (mat. 1)	0.00000E+00	0.00000E+00	0.00000E+00
	^{238}U (mat. 1)	0.00000E+00	0.00000E+00	0.00000E+00
	^{235}U (mat. 2)	–2.95972E-01	–1.60073E-06	0.00000E+00
	^{238}U (mat. 2)	4.18773E-02	–2.20723E-04	0.00000E+00
	^{16}O	–1.68307E-02	–4.44648E-04	0.00000E+00

(a) For example, this number is the second derivative of the leakage with respect to the ^{238}U source emission rate for the 1.001-MeV line and the ^{235}U cross section in material 1. Note that it is the same as the number footnoted in Table VII.

Table IX. Second-Order Sensitivities (Absolute) of the Leakage to Material Densities and Isotopic Parameters.

Parameter	ρ_1	ρ_2
^{235}U N (mat. 1)	9.35962E-01	9.64081E+00
^{238}U N (mat. 1)	–3.28783E-01	–2.57589E+00
^{235}U N (mat. 2)	–1.09878E-01[(a)]	1.18215E+03
^{238}U N (mat. 2)	–1.09878E-01	–1.56906E+02
^{16}O N	–6.24832E-03	6.72238E+01
^{235}U σ (mat. 1)	–2.37678E-05	3.12811E-03
^{238}U σ (mat. 1)	–9.38703E-05	1.23544E-02
^{235}U σ (mat. 2)	–5.94264E-07	–1.63448E-04
^{238}U σ (mat. 2)	–8.19425E-05	–2.25377E-02
^{16}O σ	–1.65073E-04	–4.54023E-02
^{235}U q (mat. 1)	0.00000E+00	0.00000E+00
^{238}U q (mat. 1)	1.41002E-08	–1.15252E-05
^{235}U q (mat. 2)	0.00000E+00	0.00000E+00
^{238}U q (mat. 2)	0.00000E+00	1.28982E-05
^{16}O q	0.00000E+00	0.00000E+00
ρ_1	–1.85783E-04	–2.72924E-04
ρ_2	–2.72924E-04	–2.85848E-02

(a) For example, this number is the second derivative of the leakage with respect to the ^{235}U atom density in material 2 and the mass density of material 1.

VII. Summary and Future Work

In this memo, the equations derived in Ref. 1 for second-order sensitivities of a detector response to uncollided particles are solved and the inner products are evaluated using ray-tracing. Results for a homogeneous sphere are in excellent agreement with analytic results as well as PARTISN results presented in Ref. 2. Results for a two-region slab are presented in anticipation of a future analytic solution. The detector response is the partial current density at a point on the surface. For the sphere, this can be integrated over the surface to yield the total leakage. For the slab, the point is on the "right" surface and it yields the total leakage through the right surface.

Also in this memo, analytic formulas for the total leakage from a homogeneous sphere[4,5] and the scalar flux at a point on the surface of a homogeneous sphere,[12] which are derived in different ways in the literature, are derived using ray-tracing.

In the future, the SENSPG code will be extended to compute second-order sensitivities of interface locations, including mixed partial derivatives of interface locations and the isotopic quantities (number density, cross section, and source emission rate).

Acknowledgments

This work was funded by the United States National Nuclear Security Administration's Office of Defense Nuclear Nonproliferation Research & Development. The author wishes to thank Ed Vigil (Los Alamos National Laboratory, CPA-CAS) for drawing Figs. 1 and 2.

References

1. Dan Gabriel Cacuci, "Second-Order Sensitivity Analysis of Uncollided Particle Contributions to Radiation Detector Responses," April 25, 2017.

2. Dan Gabriel Cacuci and Jeffrey A. Favorite, "Second-Order Sensitivity Analysis of Uncollided Particle Contributions to Radiation Detector Responses," *Nuclear Science and Engineering*, submitted (October 10, 2017).

3. R. E. Alcouffe, R. S. Baker, J. A. Dahl, E. J. Davis, T. G. Saller, S. A. Turner, R. C. Ward, and R. J. Zerr, "PARTISN: A Time-Dependent, Parallel Neutral Particle Transport Code System," Los Alamos National Laboratory report LA–UR–08-7258 (Revised September 2017).

4. K. M. Case, F. de Hoffmann, and G. Placzek, *Introduction to the Theory of Neutron Diffusion, Vol. 1*, Los Alamos Scientific Laboratory Report, United States Atomic Energy Commission (1953).

5. J. J. Duderstadt and L. J. Hamilton, *Nuclear Reactor Analysis*, Chap. 4, John Wiley & Sons, New York (1976).

6. Jeffrey A. Favorite, Keith C. Bledsoe, and David I. Ketcheson, "Surface and Volume Integrals of Uncollided Adjoint Fluxes and Forward-Adjoint Flux Products," *Nuclear Science and Engineering*, **163**, *1*, 73-84 (2009). DOI: 10.13182/NSE163-73.

7. Jeffrey A. Favorite, "Adjoint-Based Constant-Mass Partial Derivatives," *Annals of Nuclear Energy*, **110**, 1052-1059 (2017). DOI: 10.1016/j.anucene.2017.08.015

8. Eric W. Weisstein, "Directional Derivative," from MathWorld–A Wolfram Web Resource. http://mathworld.wolfram.com/DirectionalDerivative.html

9. E. E. Lewis and W. F. Miller, Jr., *Computational Methods of Neutron Transport*, Chap. 1-6, American Nuclear Society, Inc., La Grange Park, Illinois (1993).

10. J. J. Duderstadt and W. R. Martin, *Transport Theory*, Chap. 2.1.6, John Wiley & Sons, New York (1979).

11. www.wolframalpha.com, accessed Aug. 29, 2017.

12. A. B. Chilton, J. K. Shultis, and R. E. Faw, *Principles of Radiation Shielding*, Chap. 6.4.4, Prentice-Hall, Englewood Cliffs, New Jersey (1987).

13. R. Piessens, E. Dedoncker-Kapenga, C. Ueberhuber, and D. Kahaner, *QUADPACK: A Subroutine Package for Automatic Integratio*n, Springer-Verlag, New York (1983); available on the Internet at http://people.scs.fsu.edu/~burkardt/f_src/quadpack/quadpack.html; www.netlib.org

14. Keith C. Bledsoe, Jeffrey A. Favorite, and Tunc Aldemir, "Using the Levenberg-Marquardt Method for Solutions of Inverse Transport Problems in One- and Two-Dimensional Geometries," *Nuclear Technology*, **176**, *1*, 106-126 (2011). DOI: 10.13182/NT176-106.

15. R. Gunnick and J. F. Tinney, "Analysis of Fuel Rods by Gamma-Ray Spectroscopy," Lawrence Livermore National Laboratory report UCRL-51086, Appendix C (August 1971).

JAF:jaf

Distribution:
R. C. Little, XCP-DO, MS B218, rcl@lanl.gov
A. Sood, XCP-3, MS F663, sooda@lanl.gov
C. J. Werner, XCP-3, MS F663, cwerner@lanl.gov
R. J. Zerr, CCS-2, MS D409, rzerr@lanl.gov
B. A. Temple, XTD-NTA, MS T082, temple@lanl.gov
S. A. Turner, XTD-NTA, MS T082, turners@lanl.gov
E. F. Shores, XTD-SS, MS T082, eshores@lanl.gov
K. L. Buescher, XCP-8, MS F605, klb@lanl.gov
E. A. McKigney, XCP-3, MS F663, mckigney@lanl.gov
C. J. Solomon, XCP-3, MS F663, csolomon@lanl.gov
J. A. Favorite, XCP-3, MS F663, fave@lanl.gov
XCP-3 File
X-archive

APPENDIX A
SENSPG INPUT FILES

SENSPG Input File for Sec. V

```
simple sphere
sphere ptflux
mendf71x
1 / no of materials
1 94239 0.94        94240 0.06        /
15.8      / densities
1 / no of shells
 3.794         / radii
 1           / material nos
 1          / index of coarse mesh to use for reaction rates
 0          / number of reaction-rate ratios
```

SENSPG Input File for Sec. VI

```
two-region slab
slab ptflux
mendf71x
2 / no of materials
1 92235 0.20        92238 0.80        /
2 92235 6.267397832E-03 92238 8.752600761E-01  8016 1.184725261E-01 /
18.8  10. / densities
2 / no of regions
0.  4.   10.      / interface locations
    1     2       / material nos
 1          / index of coarse mesh to use for reaction rates
 0          / number of reaction-rate ratios
```